J. Microbiol. Biotechnol. (2008), **18**(1), 48–54

JOURNAL OF MICROBIOLOGY AND BIOTECHNOLOGY

Identification of ω-Aminotransferase from *Caulobacter crescentus* and Site-directed Mutagenesis to Broaden Substrate Specificity

Hwang, Bum-Yeol[1†], Seung-Hyun Ko[1], Hyung-Yeon Park[2], Joo-Hyun Seo[1], Bon-Su Lee[2], and Byung-Gee Kim[1*]

[1]*School of Chemical Engineering, and Institute for Molecular Biology and Genetics, Seoul National University, Seoul 151-742, Korea*
[2]*Division of Chemistry, Inha University, Incheon 402-751, Korea*

Received: April 20, 2007 / Accepted: August 15, 2007

A putative ω-aminotransferase gene, *cc3143* (*aptA*), from *Caulobacter crescentus* was screened by bioinformatical tools and overexpressed in *E. coli*, and the substrate specificity of the ω-aminotransferase was investigated. AptA showed high activity for short-chain β-amino acids. It showed the highest activity for 3-amino-*n*-butyric acid. It showed higher activity toward aromatic amines than aliphatic amines. The 3D model of the ω-aminotransferase was constructed by homology modeling using a dialkylglycine decarboxylase (PDB ID: 1DGE) as a template. Then, the ω-aminotransferase was rationally redesigned to increase the activity for 3-amino-3-phenylpropionic acid. The mutants N285A and V227G increased the relative activity for 3-amino-3-phenylpropionic acid to 3-amino-*n*-butyric acid by 11-fold and 3-fold, respectively, over that of wild type.

Keywords: ω-Aminotransferase, substrate specificity, homology modeling, rational design, *Caulobacter crescentus*

With complete genome sequences now available for several prokaryotic and eukaryotic organisms, biological researchers are faced with the unprecedented scientific challenges of assigning molecular and cellular functions to thousands of newly predicted gene products and explaining how these products cooperate in complex physiological processes [4, 26]. At the same time, computational structure modeling, multiple sequence analysis, and *in-vitro* evolution have become powerful tools in parallel to understand their detailed reaction functions and to find and design novel enzymes, suggesting that new integrated approaches to find such enzymes are possible and very challenging [2, 13, 25].

Aminotransferase (E.C. 2.6.1.X.) is a pyridoxal 5'-phosphate (PLP)-dependent enzyme, which is ubiquitous in nature and plays an important amino group transferring role in nitrogen metabolism in cells. Aminotransferase has many advantages over other systems such as no requirement of external addition of a cofactor, high enantioselectivity and regioselectivity, broad substrate specificity, and high reaction rate and stability [22]. Aminotransferases are classified into five subgroups on the basis of multiple sequence alignments and protein structures in Pfam (http://www.sanger.ac.uk/Software/Pfam/) [21]. Among them, aminotransferases such as acetylornithine aminotransferase, ornithine aminotransferase, ω-aminotransferase (ω-AT), 4-aminobutyrate aminotransferase, and so on, in subgroup "aminotransferase class III" are especially useful for the synthesis of non-natural amino acids and optically pure amines, which are now in burgeoning demand as intermediates for the synthesis of peptidomimetic pharmaceuticals and in combinatorial synthesis [9].

Development of bioinformatics and functional genomics makes it possible to screen many desirable aminotransferases with the help of computational techniques from the aminotransferase databases. We can predict approximate functions and substrate specificities of putative enzymes using BLAST search, multiple sequence alignment, family profile analysis, 3D structure modeling, and computer simulation of substrate docking into the active site of the enzyme. Rational protein design by site-directed mutagenesis is one of the most effective strategies to elaborate improved enzymes. Reshaping a substrate-binding site [5], substrate specificity [14], cofactor specificity [23], enantioselectivity [16], and stability [15] are achievable when a good three-dimensional structure is available. A rational approach may also work from a reasonable model derived from

*Corresponding author
Phone: 82-2-880-6774; Fax: 82-2-883-6020;
E-mail: byungkim@snu.ac.kr

†Current Address: Institute for Cellular and Molecular Biology and Department of Chemical Engineering, University of Texas, Austin, TX 78712, U.S.A.

sequence homology and molecular modeling [1]. Homology modeling is a powerful tool to predict the unknown 3D structure of the desired protein based on the proteins whose structures are known to be homologous to it [7].

Previously, we reported on screening by traditional methods and characterization of two ω-ATs from *Vibrio fluvialis* [20] and *Alcaligenes denitrificans* [24], and their applications to synthesis of chiral amines and short-chain aliphatic β-amino acids [19]. In this study, we screened a putative ω-AT from *Caulobacter crescentus* by bioinformatical tools and investigated the substrate specificity. We also tried to rationally redesign the ω-AT to increase the activity toward aromatic β-amino acid.

MATERIALS AND METHODS

Bacterial Strains, Plasmids, and Culture Condition

Bacterial strains and plasmids used in this study are listed in Table 1. *E. coli* cells were grown at 37°C in Luria-Bertani (LB) medium with shaking or on LB medium supplemented with 1.5% agar. When needed, kanamycin was added at 50 μg/ml. Plasmid DNA was purified using a plasmid prep kit from NucleoGen (Ansan, Korea).

Chemicals and Enzymes

L-Homoleucine and L-homoisoleucine were purchased from Fluka (Buchs, Switzerland). 3-Amino-3-phenylpropionic acid, 3-amino-*n*-butyric acid, various amines, and pyruvate were purchased from Sigma-Aldrich Chemicals Co. (St. Louis, MO, U.S.A.). HPLC-grade methanol was obtained from Duksan Chemical Co. (Ansan, Korea). Other chemicals were obtained from Sigma-Aldrich Chemicals Co. (St. Louis, MO, U.S.A.) and were the highest grade available. Restriction enzymes, DNA-modifying enzymes and other molecular reagents were obtained from New England Biolabs (Beverly, MA, U.S.A.), Roche Biochemical (Indianapolis, IN, U.S.A.), Quiagen (Hilden, Germany), Novagen (Darmstadt, Germany), and Genenmed (Pittsburg, PA, U.S.A.).

Construction of the Expression Vector pJCC3143

The expression plasmid pJCC3143 encoding for a putative ω-AT from *C. crescentus* was constructed as follows. The primers for the ω-AT (5'-GGATGCTGCATATGCCCGATTTCGGCGCCA-3' and 5'-CTAAGGGATCCCTAATCGACCTGACCCAGC-3') (restriction sites are underlined), which were modified to contain NdeI-BamHI recognition sites to facilitate cloning in frame into expression vector pET24ma, were synthesized. These primers were used to amplify 1,320-bp DNA fragment from a genomic DNA of *C. crescentus* CB15. PCR was carried out in a GeneAmp PCR 2400 (Perkin-Elmer) with 30 cycles of denaturation for 30 sec at 94°C, annealing for 30 sec at 55°C, and extension for 60 sec at 72°C, followed by a 5 min extension period at 72°C. The amplified PCR products were digested by NdeI-BamHI and the resulting fragments were inserted into the corresponding sites of pET24ma. The pJCC3143 was sequenced to confirm that the sequences of the inserts were identical to that of the ω-AT gene.

Site-directed Mutagenesis

Mutations were introduced into the plasmid pJCC3143 with a PCR-based technique using *Pfu* polymerase, an enzyme with proofreading activity. The primers used to create mutants of the ω-AT are described in Table 1. The PCR amplifications were treated with DpnI and propagated into *E. coli* DH5α cells. The resulting plasmids were sequenced to confirm the DNA sequences of the open reading frames of mutated genes. All mutated recombinant plasmids were transformed into *E. coli* BL21 (DE3) for expression of the recombinant proteins.

Overexpression of ω-AT in *E. coli*

For overexpression of the ω-AT, *E. coli* BL21 (DE3) were transformed with pJCC3143. The resulting transformants were grown in LB medium (containing 50 μg/ml of kanamycin) at 37°C until the optical density at 600 nm was 0.6. Then, they were induced with 0.6 mM isopropyl-β-D-thiogalactopyranoside (IPTG) at 37°C for 6 h. Cells were harvested by centrifugation at 7,000 ×*g* for 15 min at 4°C. The cell pellets were washed with phosphate-

Table 1. *E. coli* strains, chromosomal DNA, plasmids, and primers used in this study.

Strain or plasmid	Relevant properties[a]	Source or reference
Strains		
DH5α	F⁻ ϕ80*lacZ* M15 *endA recA hsdR*($r_K^-m_K^-$) *supE thi gyrA relA* Δ(*lacZYA-argF*)U169	Laboratory stocks
BL21 (DE3)	F⁻ *ompT hsdS*$_B$ ($r_B^-m_B^-$) *gal dcm*	Novagen
Genomic DNA		
C. crescentus CB15	Wild type	ATCC 19089D
Plasmids		
pET24ma	p15A replication origin, T7 lac promoter; C-terminal His-tag coding, kan^R	Sourdive D.
pJCC3143	pET24ma carrying PCR product of *apt.A* from *C. crescentus* chromosomal DNA	This work
Primers		
V227G forward	5'-TCAACGGGC**GGC**CTGATTCCGCCGAAG-3'	This work
V227G reverse	5'-CGGAATCAG**GCC**GCCCGTTGAACCGGC-3'	This work
R260L forward	5'-GGCTTTGGA**CTG**GTCGGCGCGCCGTTC-3'	This work
R260L reverse	5'-CGCGCCGAC**CAG**TCCAAAGCCGGTGAT-3'	This work
N285A forward	5'-GGCCTGACC**GCC**GCCGCCGTGCCCTGC-3'	This work
N285A reverse	5'-CACGGCGGC**GGC**GGTCAGGCCCTTGGC-3'	This work

[a]Bold and underlined letters indicate mutated bases.

buffered saline (PBS) buffer (pH 7.5). Cells were resuspended in 50 mM phosphate buffer (pH 7.5) containing 2 mM of EDTA, 1 μM of phenylmethanesulfonyl fluoride (PMSF), 20 μM of PLP, and 0.01% (v/v) of 2-mercaptoethanol. The cells were then disrupted by sonication, and the cell debris was removed by centrifugation at 14,000 ×*g* for 30 min at 4°C and the resulting supernatant was dialyzed against 1 l of the dialysis buffer composed of 50 mM phosphate buffer (pH 7.5), 20 μM PLP, 0.2 mM EDTA, 1 μM PMSF, 10% (w/v) glycerol, and 0.001% (v/v) 2-mercaptoethanol.

Enzyme Assays

For the investigation of the ω-AT activity, the 500 μl of assay mixture contained 50 mM phosphate buffer (pH 7.5), 10 mM amines or β-amino acids as amino donor, 10 mM pyruvate as amino acceptor, 20 μM PLP, and the enzyme. For racemic amino donors, the concentration of amino donor was 20 mM. The reaction was started by the addition of recombinant enzyme, and the decrease of the substrate pyruvate was measured using an HPLC system (Waters 660, U.S.A.) equipped with an AmineX HPX-87H column from Bio-rad (Hercules, CA, U.S.A.) after stopping the reaction by adding 16% perchloric acid. The mobile phase was 5 mM H_2SO_4 aqueous solution at a flow rate of 0.6 ml/min. UV detection at 210 nm was used for quantification at the ambient temperature. The 2,3,4-tetra-*O*-acetyl-β-D-glucopyranosyl isothiocyanate (GITC) derivatization method was also applied to analyze the chirality of the β-amino acids and amines [7]. After derivatization, the analytes were eluted with a mixture of 40% methanol and 60% 10 mM phosphate buffer (pH 1.8) at a flow rate of 1.0 ml/min and detected at 254 nm. One unit of the enzyme activity was defined as the amount of the enzyme that catalyzes the formation of 1 μmol of L-alanine from 20 mM racemic 3-amino-*n*-butyric acid and 10 mM pyruvate for 1 min.

Homology Modeling and Substrate Docking

A homology model of the ω-AT from *C. crescentus* was constructed based upon the known structure of 2,2-dialkylglycine decarboxylase (PDB code 1DGE) as template using the Composer and Genefold module in SYBYL 6.8 (Tripos, St. Louis, MO, U.S.A.). The PLP molecule was taken from the 2,2-dialkylglycine decarboxylase structure and included in the model as a hetero atom during the homology modeling. Manual adjustments were made to remove steric crashes of the side chain torsion angles of residues using the Homology module in SYBYL 6.8. Calculation of the accessible surface area of the substrates was carried out with the SYBYL 6.8 program as follows. The initial structures of the substrates were created by using SYBYL 6.8. The initial structures of the substrates were energy-minimized using conjugate gradient minimization until the maximum derivative was less than 0.001 kcal/mol/Å. In all minimizations, a cutoff distance of 13 Å was used with the Tripos Force Field using the Gasteiger-Huckel charge. With the energy-minimized conformers of the substrates, solvent-accessible surface areas of a subgroup of the substrates were calculated using Connolly's method with a probe size of 1.4 Å. The energy-minimized conformers of the substrates were also docked into the active site using the FlexX program (Tripos, St. Louis, MO, U.S.A.). The active site binding pocket was determined with the MOLCAD surface program (Tripos, St. Louis, MO, U.S.A.).

Results

Identification of the Putative ω-AT in *C. crescentus*

Previously, we screened an ω-AT (AptA) from *A. denitrificans* (AAP92672) from a soil sample, and cloned and characterized it [24]. Homology analysis of the deduced amino acid sequence of the AptA from *A. denitrificans* with the NCBI protein database using BLAST searches revealed that the enzyme showed high similarity with a putative ω-AT Cc3143 (AptA) from *Caulobacter crescentus* (GenBank Accession No. AAK25105; 65% identity and 77% similarity). The genome of *C. crescentus*, a Gram-negative bacterium that grows in dilute aquatic environment, has been completely sequenced [12], providing the data necessary for designing primers complementary to the regions flanking the putative ω-AT gene of this species. AptA from *C. crescentus* showed high similarity with Tlr0408 from *Thermosynechococcus elongatus* (GenBank Aceession No. NP681198; 64% identity) [11], SMc01534 from *Sinorhizobium meliloti* (GenBank Accession No. NP386510; 62% identity) [3], Mll1632 from *Mesorhizobium loti* (GenBank Accession No. NP103175; 62% identity) [10], and RSp1056 from *Ralstonia solanacearum* (GenBank Aceession No. NP522617; 56% identity) [18]. The linear alignment of these ω-ATs shows that these are highly homologous to each other (Fig. 1).

Cloning and Overexpression of AptA

The *aptA* of *C. crescentus* encoding a putative ω-AT was cloned into pET24ma containing the T7 promoter. The ω-AT was overexpressed in a soluble form in *E. coli* BL21 (DE3) by IPTG induction for 6 h at 37°C. AptA was expressed in a soluble form in *E. coli* BL21 (DE3) by IPTG induction for 6 h at 37°C. The expression was confirmed by SDS-polyacrylamide gel electrophoresis (PAGE) (Fig. 2). The molecular mass of the ω-AT was about 48 kDa in SDS-PAGE gel, which agreed well with the molecular mass (47,628 Da) deduced from the nucleotide sequence.

ω-AT Reaction

The substrate specificity of the recombinant enzyme was examined with β-amino acids, aliphatic amines, and aromatic amines (Table 2). The reaction was started by addition of the dialyzed cell extract with recombinant enzyme. We also prepared the dialyzed cell extract of *E. coli* BL21 (DE3) with native pET24ma and carried out the aminotransferase reaction with it as a negative control. We found that the aminotransferase reaction by the dialyzed cell extract of *E. coli* BL21 (DE3) with native pET24ma was negligible. AptA showed high activity for short-chain β-amino acids. It showed the highest activity for 3-amino-*n*-butyric acid. 3-Amino-*n*-butyric acid was 1.1-fold more reactive than β-alanine, which is generally one of the most reactive amino donors for the ω-AT. The activity for 3-amino-*n*-butyric

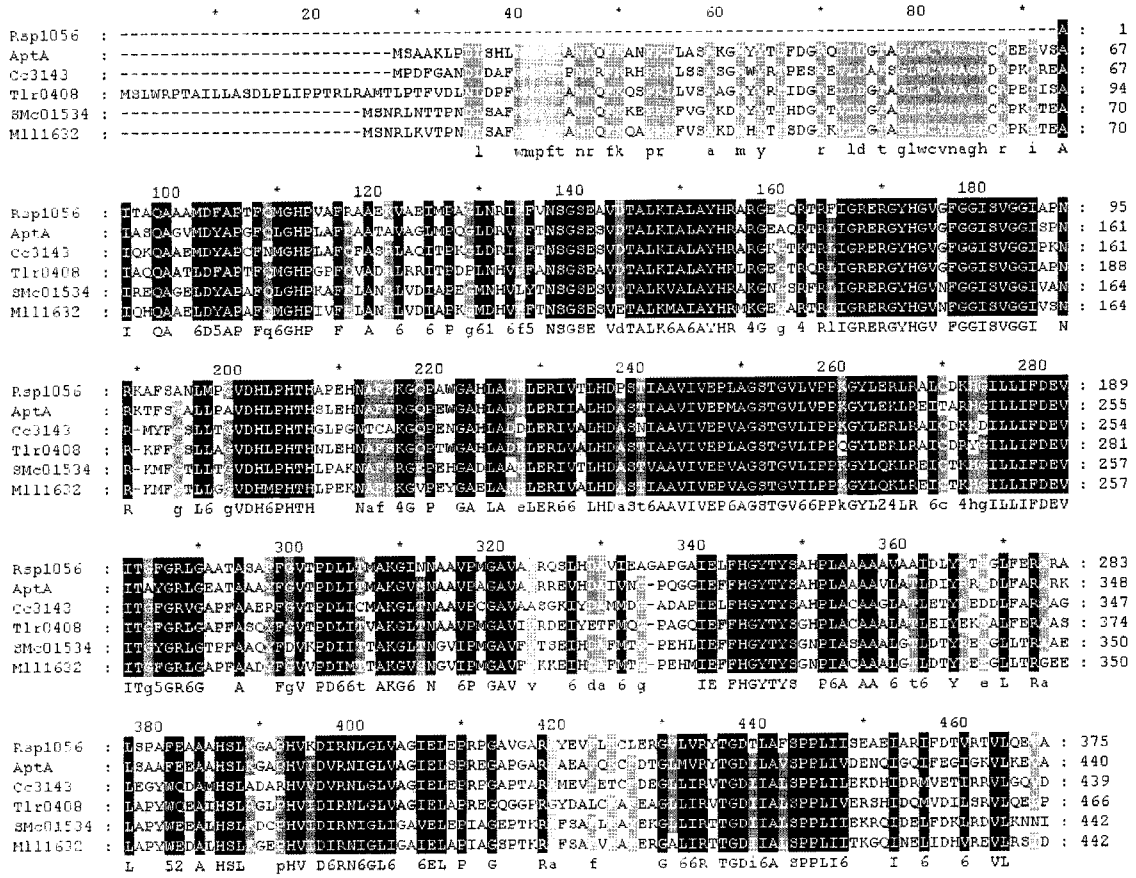

Fig. 1. Sequece alignment of AptA and other related proteins.
Introduced gaps are shown with hyphens. Highly conserved residues are highlighted in black, and less strongly conserved residues are in gray boxes. Proteins: Rsp1056 from *Ralstonia solanacearum* (gi, 17549277); AptA from *Alcaligenes denitrificans* (gi, 33086798); Cc3143 from *Caulobacter crescentus* (gi, 13424809); Tlr0408 from *Thermosynechococcus elongatus* (gi, 22297951); SMc01534 from *Sinorhizobium meliloti* (gi, 15966157); Mll1632 from *Mesorhizobium loti* (gi, 13471609).

acid was 37 mU/μl. The ω-AT from *A. denitrificans* also showed the highest activity for 3-amino-*n*-butyric acid, which is higher than that for β-alanine by 10-fold [24]. In the case of AptA, the ratio of the activity between 3-amino-*n*-butyric acid and β-alanine was not so big in comparison with the ω-AT from *A. denitrificans*. It showed low activity for long-chain aliphatic β-amino acids such as L-β-homoleucine and L-β-homoisoleucine, and for aromatic β-amino acids such as 3-amino-3-phenylpropionic acid. It showed higher activity toward aromatic amines than aliphatic amines. In the case of amino acceptor, pyruvate showed high activity, whereas oxaloacetate and α-ketoglutarate were inert. The enzyme showed (*S*)-enantioselectivity toward DL-β-amino-*n*-butyric acid and α-methylbenzylamine, and the enantiomeric ratios were all above 50. The high enantioselectivity was beneficial for preparation of enantiopure β-amino-acids and amines *via* kinetic resolution.

The enzyme activity versus pH was determined within a pH range of 5.0 to 9.5 with 20 mM racemic 3-amino-*n*-butyric acid as an amino donor and 10 mM pyruvate as an amino acceptor at 37°C. A reaction buffer containing 100 mM sodium acetate (pH 5.0 to 6.0), 100 mM potassium phosphate (pH 6.0 to 8.0), and 100 mM boric acid (pH 8.0–9.5) was used for the enzyme assay. The optimum pH of the enzyme was identificed as *ca.* 8.5 (data not shown).

Homology Modeling

In order to construct the structural model of the AptA, the selection of a template structure that has high sequence similarity with the AptA is the first requirement. The rationales to select the template sequence in this study were sequence-wide and reaction-wide similarity. First, homology analysis of AptA using the NCBI PDB database and BLAST search revealed 7,8-diaminopelargonic acid synthase from *E. coli* (PDB ID: 1QJ5), γ-aminobutyrate aminotransferase from *E. coli* (PDB ID: 1SFF), glutamate-1-semialdehyde aminomutase from *Synechococcus* sp. (PDB ID: 3GSB), ornithine aminotransferase from *Homo sapience* (PDB ID: 1OAT), and dialkylglycine decarboxylase from *Burkholderia cepacia* (PDB ID: 1DGE). All these enzymes including AptA belong to the subgroup "aminotransferase class III" in the Pfam database. Among these five structures, the sequence alignment using Genefold (Tripos, St. Louis, MO, U.S.A.) revealed dialkylglycine

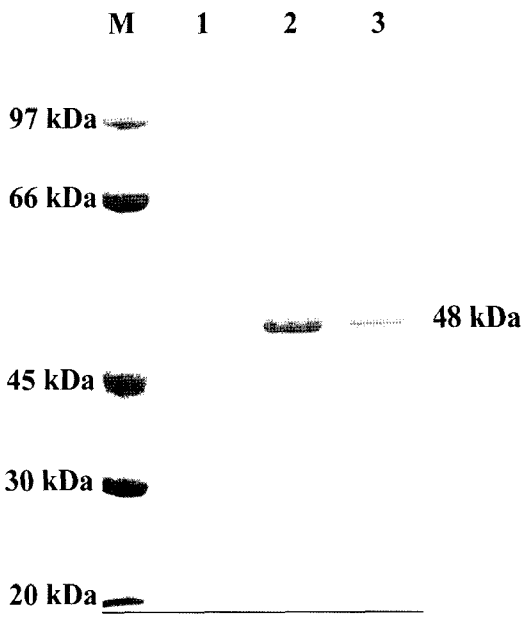

Fig. 2. Expression of *aptA* in *E. coli* BL21 (DE3) examined by SDS-PAGE analysis.
Lane M, molecular size marker proteins; lane 1, total cell extract of *E. coli* BL21 (DE3) containing pET24ma; lane 2, total cell extract of *E. coli* BL21 (DE3) expressing AptA; lane 3, soluble fraction of cell extract of *E. coli* BL21 (DE3) expressing AptA.

decarboxylase from *Burkholderia cepacia* (PDB ID: 1DGE) to have the highest similarity with AptA. Moreover, the molecular structures of one of the reaction substrates and one of the reaction products of dialkylglycine decarboxylase are similar to those of AptA in that they use pyruvate as a substrate and produce alanine as a product. Therefore, it was used as the template structure for homology modeling of AptA.

The homology model of AptA was constructed by the Composer and Genfold+ module in SYBYL 6.8. The PLP molecule was taken form the 2,2-dialkylglycine decarboxylase structure and included in the model as a hetero atom during the homology modeling. Manual adjustments were made to remove steric crashes of the side chain torsion angles of residues using the Homology module in SYBYL 6.8.

Aminotransferase has a catalytic lysine that forms a Schiff base with the PLP, and aspartate or glutamate that forms a salt bridge with the pyridine N-1 of the PLP in the active site [8]. The phosphate group of the PLP is stabilized by hydrogen bonds with the highly conserved residues such as serine, tyrosine, arginine, aspartate, and threonine in the active site. The large binding pocket is enclosed by Thr49, Ile52, Trp53, Gly223, Ile255, Arg260, Val374, and Ser414. The small binding pocket is composed of Ser224, Thr225, Gly226, Val227, Arg405, Thr407, Ile410, Ile411, and Ala412 (Fig. 3).

Table 2. The amino donor specificity of ω-AT AptA from *C. crescentus*.[a]

Amino donor	Relative activity (%)[b]
Benzylamine	100
(*S*)-α-Methylbenzylamine	169
(*R,S*)-α-Ethylbenzylamine	156
L-Phenylglycine	3
2-Phenylethylamine	75
3-Phenyl-1-propylamine	88
Ethylamine	21
1-Propylamine	12
1-Butylamine	15
Isopropylamine	24
(*R,S*)-*sec*-Butylamine	6
(*R,S*)-*sec*-Amylamine	10
β-Alanine	290
D,L-3-Amino-*n*-butyric acid	312
L-β-Homoleucine	3
L-β-Homoisoleucine	5
D,L-3-Amino-3-phenylpropionic acid	1

[a]Pyruvate (10 mM) and 10 mM each amino donor were used, and the initial reaction rate was measured by analyzing the amount of pyruvate consumed. The activity for benzylamine, corresponding to 12 mU/μl, was taken as 100%. For racemic amino donors, the concentration of amino donor was 20 mM.

Site-directed Mutagenesis

We carried out the site-directed mutagenesis to increase the activity for 3-amino-3-phenylpropionic acid. According to the predicted structure of AptA, the small binding pocket is not enough large to accept the phenyl group of 3-amino-3-phenylpropionic acid. The key rationale is the enlargement of the small binding pocket. Among the residues that make

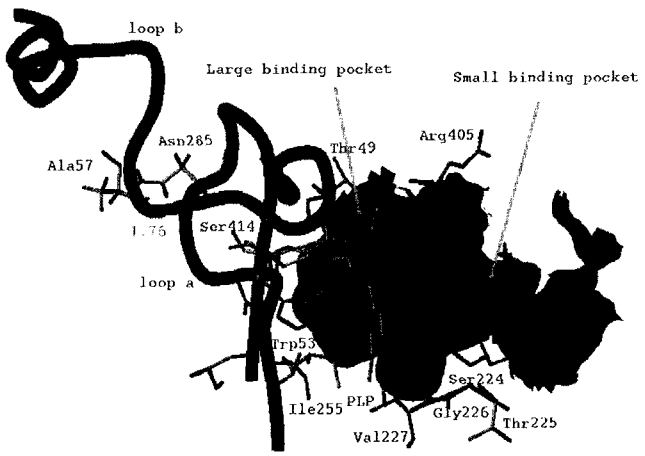

Fig. 3. The proposed structure around the active site binding pocket of the 3D model of AptA constructed by homology modeling.
The large binding pocket is enclosed by Thr49, Ile52, Trp53, Gly223, Ile255, Arg260, Val374, and Ser414. The small binding pocket is composed of Ser224, Thr225, Gly226, Val227, Arg405, Thr407, Ile410, Ile411, and Ala412. The distance between NH_2 of Ala57 and C=O of the side chain of Asn285 is 1.76 Å.

Table 3. The amino donor specificity of the mutants of ω-AT AptA from *C. crescentus*.

Mutant	Specific activity (mU/μl)[a]		Ratio of activity (3A3PPA/3AB) (%)
	3AB[b]	3A3PPA[c]	
Wild type	12	0.038	0.3
V227G	6.7	0.09	1.3
R260L	0.4	n.d.[d]	n.d.[d]
N285A	3.3	0.11	3.3

[a]Pyruvate (10 mM) and 20 mM each racemic amino donor were used, and the reaction was carried out by the crude enzyme extract. The conversion was measured by analyzing the amount of pyruvate consumed.
[b]3AB: 3-amino-*n*-butyric acid.
[c]3A3PPA: 3-amino-3-phenylpropionic acid.
[d]n.d.: not determined.

up the small binding pocket, Val227, whose bulky side chain was located toward the small binding pocket, was mutated into glycine to lessen the steric hindrance between the substrate and the residues positioned at the small binding pocket. Asn285 was also mutated into alanine. The Asn285 is positioned at a loop (loop a) that forms the small binding pocket and forms a hydrogen bond with Ala57 at another loop (loop b) (Fig. 3). The catalytic lysine (K281) is at the loop a. We expected that the loop a could move somewhat freely if the hydrogen bond between the loop a and the loop b was broken. If the loop a moves in the opposite direction of the active site binding, the small binding pocket could be enlarged.

Site-directed mutations were carried out by a PCR-based technique using *Pfu* polymerase. The mutants were overexpressed in *E. coli* BL21 (DE3) and the expression levels of wild type and mutants were confirmed by SDS-PAGE. The expression levels were similar among the wild type and the mutants (data not shown). The activities for reaction with 3-amino-3-phenylpropionic acid and 3-amino-*n*-butyric acid were examined (Table 3). The mutant N285A showed three times higher activity for 3-amino-3-phenylpropionic acid than the wild type. On the other hand, its activity for 3-amino-*n*-butyric acid decreased. The mutant V227G also showed two times higher activity for 3-amino-3-phenylpropionic acid than the wild type. However, the specific activities of the dialyzed cell extract of the mutants N285A and V227G for 3-amino-3-phenylpropionic acid were only 0.11 mU/μl and 0.09 mU/μl, respectively. These specific activities for 3-amino-3-phenylpropionic acid were lower than those for 3-amino-*n*-butyric acid by 74-fold and 30-fold, respectively.

We also examined the optimal pH and temperature of the mutant N285A with 20 mM racemic 3-amino-*n*-butyric acid as an amino donor and 10 mM pyruvate as an amino acceptor. The optimum temperature of the mutant N285A was 40°C, which was a little lower than that of the wild type (50°C). The optimum pH of the mutant N285A was *ca.* 9.5, which was a little higher than the wild type (*ca.* pH 8.5).

DISCUSSION

AptA showed high activity for short-chain β-amino acids and aromatic amines. However, it showed low activity for long-chain or aromatic β-amino acids and aliphatic amines. We investigated the substrate binding in the active binding pocket using the FlexX program. In terms of 3D structure, the active site of AT is composed of two binding pockets. One is large and the other is small. The amino group of the substrate is placed in the middle of the binding pockets toward the PLP. In the case of β-amino acids, the side chains containing carboxylic group are placed in the large binding pocket. We also identified this after running the docking program (data not shown). The carboxylic group of 3-amino-*n*-butyric acid was positioned in the large binding pocket. It was stabilized by the hydrogen bond with Arg260. To identify this, we mutated the arginine into leucine. The mutant R260L showed very low activity for 3-amino-*n*-butyric acid (Table 3). This means that the Arg260 is critical to the activity of AptA. The methyl group of 3-amino-*n*-butyric acid was positioned in the small binding pocket. However, the phenyl group of 3-amino-3-phenylpropionic acid is too bulky to be positioned in the small binding pocket. The calculated volume of small binding of AptA is about 60 Å^2, which is comparable to the ethyl group and the accessible surface area of phenyl is about 90 Å^2. Therefore, AptA seemed to show very low activity for 3-amino-3-phenylpropionic acid. In the case of aromatic amines, the aryl groups are placed in the large binding pocket. The calculated volume of the large binding pocket is about 160 Å^2. It is big enough to contain the bulkier group of 3-phenyl-1-propylamine, which is the biggest substrate we investigated because the accessible surface area of it is about 130 Å^2. The aryl group could interact with Trp53 and become stabilized by hydrophobic interaction. The smaller side chains of the investigated aromatic amines are hydrogen or methyl groups. Therefore, they could be placed in the small binding pocket without difficulty. However, the carboxylic group is placed in the small binding pocket in the case of L-phenylglycine. The small binding pocket could not accept the carboxylic group. Therefore, AptA showed very low activity for L-phenylglycine. In the case of aliphatic amines, the bulkier alkyl side chains could be placed in the large binding pocket. However, there was no strong interaction between the substrate and the enzyme. Therefore, AptA seemed to show moderate activity for aliphatic amines.

We rationally redesigned the ω-AT through 3D structure modeling. The specific activity for 3-amino-3-phenylpropionic acid of the mutants N285A and V227G increased by about 3-fold and 2-fold, respectively, compared with the wild-type enzyme. The mutants N285A and V227G showed lower specific activity for 3-amino-*n*-butyric acid by 4-fold and 2-fold, respectively, than the wild type. Therefore,

the mutants N285A and V227G increased the relative activity for 3-amino-3-phenylpropionic acid to 3-amino-*n*-butyric acid by 11-fold and 3-fold, respectively, than that of wild type. The change of interaction between amino acids that are located around the active site binding pocket seemed to be more effective than that of the size of side chain of an amino acid. We showed that the substrate specificity could be changed through the change of size or interaction of amino acids that are located around the active site binding pocket.

Acknowledgments

This research was partially supported by the Brain Korea 21 program of Korea and Frontier 21 program (Ministry of Commerce, Industry and Energy, Korea).

References

1. Baker, D. and A. Sali. 2001. Protein structure prediction and structural genomics. *Science* **294:** 93–96.
2. Baxter, S. M. and J. S. Fetrow. 2001. Sequence- and structure-based protein function prediction from genomic information. *Curr. Opin. Drug Discov. Devel.* **4:** 291–295.
3. Capela, D., F. Barloy-Hubler, J. Gouzy, G. Bothe, F. Ampe, J. Batut, P. Boistard, A. Becker, M. Boutry, *et al.* 2001. Analysis of the chromosome sequence of the legume symbiont *Sinorhizobium meliloti* strain 1021. *Proc. Natl. Acad. Sci. USA* **98:** 9877–9882.
4. Figeys, D. 2002. Functional proteomics: Mapping protein-protein interactions and pathways. *Curr. Opin. Mol. Ther.* **4:** 210–215.
5. Harris, A., M. Adler, J. Brink, R. Lin, M. Foehr, M. Ferrer, B. C. Langton-Webster, R. N. Harkins, and S. A. Thompson. 1998. Homologue scanning mutagenesis of heregulin reveals receptor specific binding epitopes. *Biochem. Biophys. Res. Commun.* **251:** 220–224.
6. Hwang, B.-Y., B.-K. Cho, H. Yun, K. Koteshwar, and B.-G. Kim. 2005. Revisit of aminotransferase in the genomic era and its application to biocatalysis. *J. Mol. Catalysis B Enzym.* **37:** 47–55.
7. Ito, S., A. Ota, K. Yamamoto, and Y. Kawashima. 1992. Resolution of the enantiomers of thiol compounds by reverse-phase liquid chromatography using chiral derivatization with 2,3,4-tetra-*O*-acetyl-β-D-glucopyranosyl isothiocyanate. *J. Chromatogr.* **626:** 187–196.
8. Jansonius, J. N. 1998. Structure, evolution and action of vitamin B6-dependent enzymes. *Curr. Opin. Struct. Biol.* **8:** 759–769.
9. Kamphuis, J., E. M. Meijer, W. H. Boesten, T. Sonke, W. J. van den Tweel, and H. E. Schoemaker. 1992. New developments in the synthesis of natural and unnatural amino acids. *Ann. N. Y. Acad. Sci.* **672:** 510–527.
10. Kaneko, T., Y. Nakamura, S. Sato, E. Asamizu, T. Kato, S. Sasamoto, A. Watanabe, K. Idesawa, A. Ishikawa, *et al.* 2000. Complete genome structure of the nitrogen-fixing symbiotic bacterium *Mesorhizobium loti*. *DNA Res.* **7:** 331–338.
11. Nakamura, Y., T. Kaneko, S. Sato, M. Ikeuchi, H. Katoh, S. Sasamoto, A. Watanabe, M. Iriguchi, K. Kawashima, *et al.* 2002. Complete genome structure of the thermophilic cyanobacterium *Thermosynechococcus elongatus* BP-1. *DNA Res.* **9:** 123–130.
12. Nierman, W. C., T. V. Feldblyum, M. T. Laub, I. T. Paulsen, K. E. Nelson, J. A. Eisen, J. F. Heidelberg, M. R. Alley, N. Ohta, *et al.* 2001. Complete genome sequence of *Caulobacter crescentus*. *Proc. Natl. Acad. Sci. USA* **98:** 4136–4141.
13. Norin, M. and M. Sundstrom. 2002 Structural proteomics: Developments in structure-to-function predictions. *Trends Biotechnol.* **20:** 79–84.
14. Onuffer, J. J. and J. F. Kirsch. 1995. Redesign of the substrate specificity of *Escherichia coli* aspartate aminotransferase to that of *Escherichia coli* tyrosine aminotransferase by homology modeling and site-directed mutagenesis. *Protein Sci.* **4:** 1750–1757.
15. Perl, D., U. Mueller, U. Heinemann, and F. X. Schmid. 2000. Two exposed amino acid residues confer thermostability on a cold shock protein. *Nat. Struct. Biol.* **7:** 380–383.
16. Rotticci, D., J. C. Rotticci-Mulder, S. Denman, T. Norin, and K. Hult. 2001. Improved enantioselectivity of a lipase by rational protein engineering. *Chembiochem* **2:** 766–770.
17. Sacchi, S., S. Lorenzi, G. Molla, M. S. Pilone, C. Rossetti, and L. Pollegioni. 2002. Engineering the substrate specificity of D-amino-acid oxidase. *J. Biol. Chem.* **277:** 27510–27516.
18. Salanoubat, M., S. Genin, F. Artiguenave, J. Gouzy, S. Mangenot, M. Arlat, A. Billault, P. Brottier, J. C. Camus, *et al.* 2002. Genome sequence of the plant pathogen *Ralstonia solanacearum*. *Nature* **415:** 497–502.
19. Shin, J.-S. and B.-G. Kim. 2001. Comparison of the ω-transaminases from different microorganisms and application to production of chiral amines. *Biosci. Biotechnol. Biochem.* **65:** 1782–1788.
20. Shin, J.-S., H. Yun, J.-W. Jang, I. Park, and B.-G. Kim. 2003. Purification, characterization, and molecular cloning of a novel amine:pyruvate transaminase from *Vibrio fluvialis* JS17. *Appl. Microbiol. Biotechnol.* **61:** 463–471.
21. Sonnhammer, E. L., S. R. Eddy, and R. Durbin 1997. Pfam: A comprehensive database of protein domain families based on seed alignments. *Proteins* **28:** 405–420.
22. Taylor, P. P., D. P. Pantaleone, R. F. Senkpeil, and I. G. Fotheringham. 1998. Novel biosynthetic approaches to the production of unnatural amino acids using transaminases. *Trends Biotechnol.* **16:** 412–418.
23. Woodyer, R., W. A. van der Donk, and H. Zhao. 2003. Relaxing the nicotinamide cofactor specificity of phosphite dehydrogenase by rational design. *Biochemistry* **42:** 11604–11614.
24. Yun, H., S. Lim, B.-K. Cho, and B.-G. Kim. 2004. ω-Amino acid:pyruvate transaminase from *Alcaligenes denitrificans* Y2k-2: A new catalyst for kinetic resolution of β-amino acids and amines. *Appl. Environ. Microbiol.* **70:** 2529–2534.
25. Zhang, C. and S.-H. Kim. 2003. Overview of structural genomics: From structure to function. *Curr. Opin. Chem. Biol.* **7:** 28–32.
26. Zhu, H., M. Bilgin, and M. Snyder. 2003. Proteomics. *Annu. Rev. Biochem.* **72:** 783–812.